Journal of Applied Polymer Science

Synthesis and Application of Polyacrylate Nanocapsules Loaded with Lilial

Hu Jing, Deng Weijun, Liu Liqin, Xiao Zuobing
School of Perfume and Aroma Technology, Shanghai Institute of Technology, Shanghai 201418, People's Republic of China
Correspondence to: J. Hu (E-mail: hujing@sit.edu.cn)

ABSTRACT: Polyacrylate nanocapsules loaded with lilial (PNLs) were prepared via miniemulsion polymerization. Then, the PNLs were applied directly to leather. The influence of the contents of the surfactant and lilial and the stirring speed on the mean size and fragrance loading capacity of the PNLs was investigated in detail. The microstructure of the PNLs was determined by dynamic light scattering (DLS), transmission electron nicroscopy (TEM), Fourier transform infrared (FTIR) spectrometry, and thermogravimetric analysis (TGA). The sustained release properties of the leather finished by PNLs were characterized by scanning electron microscopy (SEM) and gas chromatography with a flame ionization detector (GC-FID). DLS showed that the mean size of the PNLs was 67.78 nm, and the polydispersity index was 0.076. TEM illustrated that the size of the spherical PNL varied in the range 30–80 nm. FTIR spectroscopy showed that lilial was encapsulated into the polyacrylate nanocapsules. TGA illustrated that the fragrance loading ratio of the nanocapsules reached 36.83%. SEM and GC-FID indicated that the leather finished by the PNLs had better flexing endurance than that finished by lilial emulsion. © 2013 Wiley Periodicals, Inc. J. Appl. Polym. Sci. **2014**, *131*, 40182.

KEYWORDS: applications; copolymers; emulsion polymerization

Received 9 May 2013; accepted 8 November 2013
DOI: 10.1002/app.40182

INTRODUCTION

Aromatic compounds play an important role in commercial activities and encourage further consumption for their pleasure and fresh odor.[1,2] However, most fragrance compounds are labile and volatile, so it is difficult to retain the stability and sustained release of the fragrance.[3] Encapsulation has been developed as an effective technique to protect these small, weakly water-soluble aromatic compounds against rapid evaporation, oxidization, and contamination. Thus, it is possible to control the volatile substance release from the enclosed capsule as required.[4,5]

Up to this point, a variety of physicochemical and chemical strategies, including spray drying, fluid bed drying, spray cooling/chilling, extrusion, molecular inclusion, coacervation, and emulsion/interfacial polymerization process, have been used to prepare microcapsules/nanocapsules.[6–9] In particular, researchers have focused on chemical technologies because of the uniform encapsulation of fragrance compounds and the excellent stability of the reaction system.[10,11] Hwang et al.[12] reported melamine–formaldehyde microcapsules containing approximately 20% peppermint oil prepared via *in situ* polymerization with Tween 20 as the emulsifier and poly(vinyl alcohol) as an additional colloidal stabilizer.[12] Zhu et al.[13] prepared perfume-encapsulating mesoporous silica spheres with a polyelectrolyte shell to control the prolonged-release of perfume by assembling 10 layers of the polyelectrolyte shell. Interestingly, Wanichwecharungruang et al.[14] fabricated a fragrance controlled release system with a thermal switch and refillability characteristics using well-accepted nontoxic biocompatible poly(ethylene oxide) and chitosan polymers. The on/off switch was modulated through the thermally induced phase separation of the fragrant spheres from the aqueous medium; this resulted in a limited efflux of the fragrant molecules from the particles.

Recently, the miniemulsion polymerization process has been shown to offer several advantages in the production of polymeric nanocapsules that cannot be achieved by other current procedures.[15,16] Theisinger et al.[17] reported the encapsulation of the hydrophobic fragrance 1,2-dimethyl-1-phenyl butyramide in poly(methyl methacrylate), polystyrene, and acrylic copolymer nanoparticles with a miniemulsion process. Different types of homopolymers and copolymers were used as the polymeric shell material with different glass-transition temperatures (T_gs) to obtain fragrance-delivery systems for long delivery time of the fragrance at different temperatures. It was shown that the amount of encapsulated volatile compound could be varied over a wide range and that the amount of the fragrance directly influenced the molecular weight, the kinetics of polymerization, and the T_g of the polymers. A combination of transmission

electron microscopy (TEM) and calorimetric experiments suggested that the particles consisted of a matrix composed of the fragrance in the polymer up to about 25% of the fragrance.

Our previous work remarkably established that the fragrance can be encapsulated into poly(butyl cyanoacrylate) nanocapsules via anionic polymerization. Although the diameters of these nanocapsules could reach 67.3 nm, the fragrance loading ratio was only 0.5%.[18] To improve the fragrance loading ratio, a complex coacervation method was used further to prepare chitosan nanoparticles loaded with 12.05% of the fragrance.[19] In this study, we successfully synthesized poly(butyl acrylate–methyl methacrylate) [P(BA–MMA)] nanocapsules with a higher loading ratio of fragrance via a one-pot miniemulsion polymerization. The effect of the contents of the surfactant and lilial and the stirring speed on the size and loading capacity of polyacrylate nanocapsules loaded with lilial (PNLs) were investigated in detail. We observed that the size and the loading capacity of fragrance could be varied over a wide range. Finally, the sustained release properties of the fragrance in leather finished by the PNLs was studied.

EXPERIMENTAL

Materials

The monomers methyl methacrylate (MMA) and *n*-butyl acrylate (BA) were distilled under reduced pressure and then kept in a refrigerator until use. The initiator potassium persulfate (KPS) was recrystallized. All of the previous chemicals were purchased from Sinopharm Group Chemical Reagent Co., Ltd. (Shanghai, China). Sodium dodecyl sulfate, *n*-hexadecane, and the lilial were supplied by Shanghai Jinchun Chemical Reagent Co., Ltd. Deionized water was used for all of the experiments.

Preparation of the PNLs

In a typical procedure, 0.3 g of sodium dodecyl sulfate, lilial (variable contents), 0.5 g of *n*-hexadecane and 80.0 g of H_2O were blended together, and an oil–water (O/W) emulsion was obtained under ultrasonic treatment at 800 W for 10 min. The previous emulsion, 1.2 g of a mixture of MMA and BA (molar ratio = 3:2) and 5 g of a KPS aqueous solution with a solid content of 0.8 wt % were charged into a 250-mL, three-necked flask equipped with a mechanical stirrer, a thermometer with a temperature controller, an N_2 inlet, a Graham condenser, and a heating mantle. This mixture was deoxygenated by bubbling nitrogen gas at room temperature for 30 min, then heated up to 75°C, and kept stirring for 30 min. Then, 4.8 g of a mixture of MMA and BA (molar ratio = 3:2) and 5 g of a KPS aqueous solution with a solid content of 3.2% were added to the flask dropwise and separately for 1 h. The polymerization was performed at 80°C for 6 h under a constant stirring rate. Then, 10 mL of cyclohexane was added to the PNL emulsion to extract the unencapsulated lilial. The mixed emulsion was held for 1 h to separate the oil phase. The obtained aqueous phase was freeze-dried to obtain the PNLs.

Dynamic Light Scattering (DLS)

The particle size of the PNLs in three replicates was determined by a Zetasizer Nano ZS (Malvern Instruments, United Kingdom). Each sample was measured by a solid state He–Ne laser of 633.0 nm at 25°C with an angle detection of 90°.

Determination of the Lilial Loading Capacity

An amount of 2 g of PNLs after freeze drying was added to 20 mL of cyclohexane. The suspension was treated with ultrasonication at 800 W for 15 min until the shell of the PNLs was destroyed and the lilial was dissolved in cyclohexane. Then, the suspension was centrifuged at a speed of 10,000 rpm for 20 min (CT15RT Versatile Refrigerated Centrifuge, Shanghai Technical Co.). The supernatant was collected in a constant weighing bottle (with a mass of W_1) and evaporated at 40°C to diminish cyclohexane under reduced pressure. The weighing bottle was placed into a desiccator to cool for 30 min and then weighed (where W_2 is the mass of the weighing bottle and the encapsulated lilial). The loading capacity (*LC*) was obtained according to the following formula, and five replicates were analyzed for the loading capacity evaluation:

$$LC(\%) = \frac{W_2 - W_1}{W} \times 100\% \quad (1)$$

where *W* is the total mass of lilial used in the reaction.

Thermogravimetric Analysis (TGA)

A TGA-Q5000IR instrument (TA Instruments) was used to measure the thermal stability of the polyacrylate nanoparticles and PNLs with different contents of lilial. This experiment was performed at temperatures from 30 to 500°C at a heating rate of 10°C/min under a constant nitrogen flow (20 mL/min). Powdered polyacrylate nanoparticles and PNLs were carried out at the same weight.

Chemical Structural Analysis

Fourier transform infrared (FTIR) spectroscopy exploits the fact that molecules absorb specific frequencies that are characteristic of their structure. The chemical structures of polyacrylate nanoparticles, lilial, and PNLs were determined with a VERTEX70 FTIR spectrophotometer (Bruker, Germany) in the range from 4000 to 600 cm^{-1}. Polyacrylate nanoparticles and PNLs after freeze drying were examined by FTIR spectroscopy.

TEM

TEM analysis was used to investigate the morphology and the diameter of the PNLs with an H-600 electron microscope (Hitachi, Japan). We obtained the TEM analysis by dropping one drop of aqueous solution containing nanoparticles onto a carbon-coated copper grid, and the sample was dried in air at room temperature without any further modification before microscopy observation.

Application of the PNLs in Leather

Leather samples (25 g) were immersed in a 10% lilial emulsion (175 g) and a 10% PNL (175 g) emulsion for 4 h at 30°C with a stirring speed of 1200 rpm. The finished leathers were then dried at 40°C with an air current rate of 0.4 m/s for 1 h in an oven (moisture content = 0.01×10^3 kg/m^3; Y802 Eight Baskets Oven, Huizhou Electricity Factory). The measurements of the flexing endurance of leather were done according to International Organization for Standardization (ISO) 5402-1:2011.

Scanning Electron Microscopy (SEM)

SEM analysis was performed on a JSM 840A scanning electron microscope (JEOL, Japan). The surface morphologies of the untreated leather, the leather finished by PNLs, and the leather

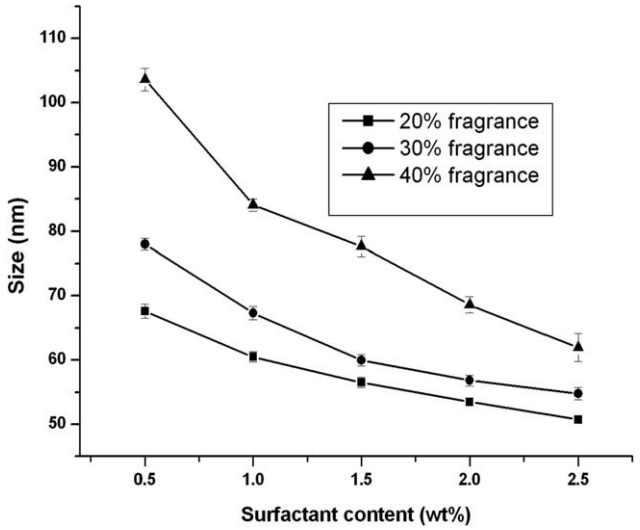

Figure 1. Relationship between the size of the PNLs and the contents of the surfactants with different lilial contents.

finished by the lilial emulsion were studied. The flexing endurance of the treated leather was also evaluated. Each leather sample was coated with a thin layer of uttered gold before examination.

Determination of the Sustained Release Properties of Fragrance in the Leather Finished by the PNLs via Gas Chromatography with a Flame Ionization Detector (GC-FID)

An Solid Phase Micro-extraction (SPME) holder (Bellefonte, PA) for manual sampling combined with an Agilent 7890A GC-FID instrument (Agilent Technologies, Inc., New York,) was used to perform the experiments. An amount of 5 g of leather finished by the lilial emulsion and PNLs for headspace analysis was normally prepared in a bottle containing both the sample and headspace. The volatile components of the sample were extracted and isolated in the headspace or gas phase in the vial. The SPME fiber was exposed to the headspace 1 cm above the aromatic leather to absorb the analytes. After 30 min, the fiber was withdrawn into a needle and then introduced into a heated chromatograph injector for desorption and analysis.

The internal standard lilial was used to measure the standard curve. An Agilent 7890A gas chromatograph was used with an HP-Innowax polar column (60 m × 0.25 mm *i.d.* × 0.25 μm film, Supelco). The carrier gas was ultrapurified helium at a flow rate of 1.0 mL/min. The initial column temperature was held at 60°C for 2 min, programmed to ramp to 150°C at a rate of 5°C/min for 5 min and then to 300°C at a rate of 5°C/min, and held at this temperature for 5 min. The FID temperature was maintained at 300°C. All measurements were carried out in triplicate, and an average value is reported.

The influence of the flexing times on the lilial released from the finished leather was investigated. The initial content of the lilial released from the finished leather without flexing was used as the initial basis (M_1). The content of those after flexing 5000 times was defined as M_2. The loss ratio (L) was calculated according to eq. (2). Analyses were performed in triplicate:

$$L(\%) = \frac{M_2 - M_1}{M_1} \times 100\% \quad (2)$$

RESULTS AND DISCUSSION

Size of the PNL

Figure 1 shows the influence of the surfactant contents on the mean size of the PNLs with lilial loadings of 20, 30, and 40%, respectively. With increasing lilial content, the size of the PNLs improved. Lilial as a hydrophobic material could only be solubilized into the micelles formed by the surfactants but was not the reactive monomer. When more lilial was added to the system, it could be diffused into the micelles directly. During the reaction process, acrylate monomers solubilized into the micelles were polymerized to encapsulate lilial via free-radical polymerization so that more lilial as the core of the nanocapsule lead to the improvement of the PNL size. Meanwhile, when the surfactants contents were enhanced, the size of the PNLs decreased. When the lilial loading was 20%, the size of the nanocapsules decreased from 68.35 to 53.21 nm. With 30% lilial loading, the size decreased from 79.78 to 58.65 nm. When 40% lilial was used, the size decreased from 105.34 to 65.65 nm. This was attributed to the fact that more surfactants could form more micelles, and the hydrophobic monomers were easily dispersed into the micelles and emulsified evenly.

Figure 2 demonstrates the influence of the stirring speed on the mean size of the PNLs at different lilial contents. The size tendency of the PNLs with lilial contents to increase was similar to the effect of the lilial contents on the particle size, as shown in Figure 1. Meanwhile, the size of the PNLs improved with increasing stirring speed. When the PNLs theoretically contained 20% lilial, the size increased from 48.96 to 73.11 nm. When 30% lilial was encapsulated, the size improved from 49.22 to 75.65 nm. In addition, when 40% lilial was used, the size increased from 52.04 to 76.60 nm. Generally, a high stirring speeds led to the enhancement of the particle size during emulsion polymerization.[12,20] With the high agitation rates, the

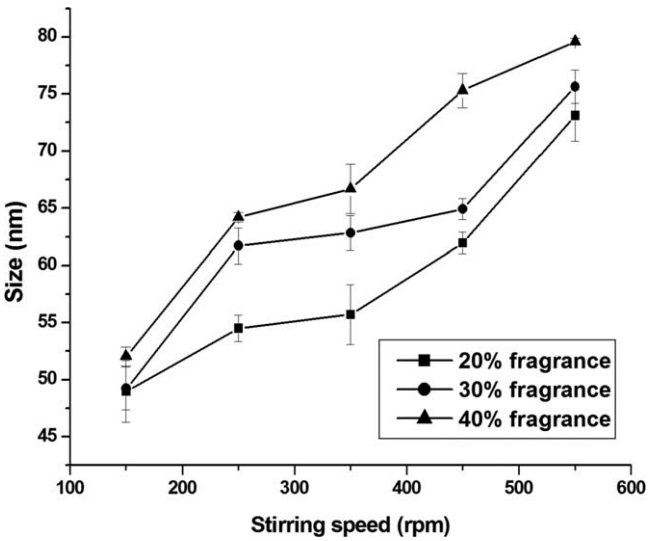

Figure 2. Relationship between the size of the PNLs and the stirring speed with different lilial contents.

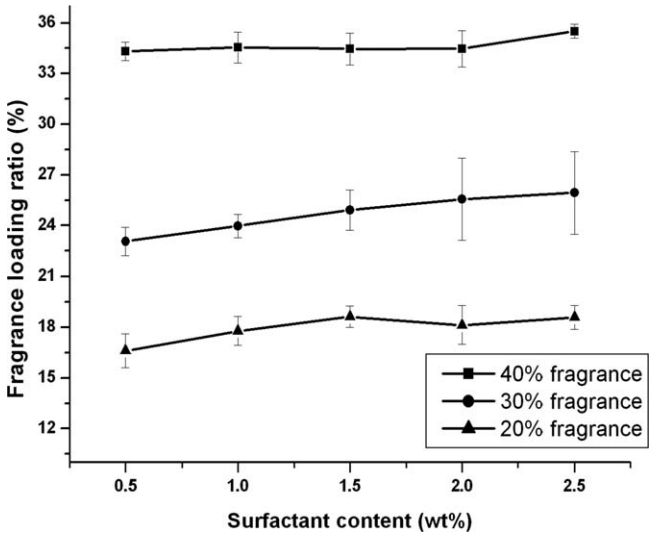

Figure 3. Relationship between the fragrance loading ratio of the PNLs and the contents of the surfactants with different lilial contents.

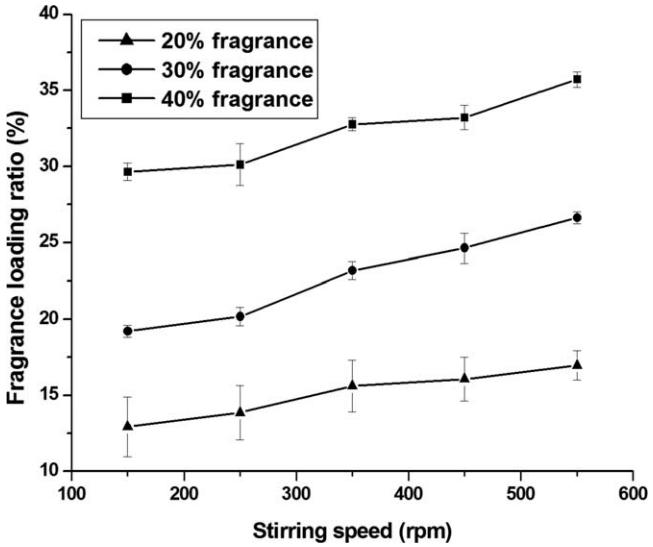

Figure 4. Relationship between the fragrance loading ratio of the PNLs and the stirring speed with different lilial contents.

emulsion particles consequently broke and reagglomerated, and also, the stability of the O/W emulsions might have decreased.

Lilial Loading Capacity

Figure 3 shows the influence of the emulsifier contents on the loading capacity of the PNLs with lilial loadings of 20, 30, and 40%, respectively. When the content of the surfactant was increased from 0.5 to 2.5%, the loading capacity of lilial in the PNLs increased. This was attributed to the fact that the emulsifiers helped lilial to be solubilized in the micelles, and acrylate monomers were initiated to be polymerized on the interface of the micelles to encapsulate the lilial. When 20% lilial was used, theoretically, the loading capacity was enhanced from 17.62 to 19.52%. The real encapsulation ratio of lilial reached 97.6%. When lilial contents of 30 and 40% were added, theoretically, the real loading capacity increased from 22.85 to 25.43% and from 34.23 to 35.78% separately. However, compared with 20% lilial in theory, the encapsulation ratio of the lilial was decreased. This was because the content of the emulsifiers was limited. There was not enough room to load the lilial.

The influence of different lilial contents and the stirring speed on the fragrance loading ratio of the PNLs is shown in Figure 4. The lilial loading ratio of the PNLs increased gradually, whereas the stirring speed improved. This was attributed the fact that the strong mechanical reaction was helpful for solubilizing more lilial into the micelle. Meanwhile, the tendency of the loading ratio of the PNLs with increasing lilial was similar to that shown in Figure 3. The fragrance loading capacity of the PNLs increased from 12.93 to 16.97%, 19.22 to 26.62%, and 29.64 to 35.72% with 20, 30, and 40% theoretical loadings, respectively. When the stirring speed was increased, the enhancement of the PNL size provided enough room to encapsulate the lilial.

TGA Results

Figure 5 displays the TGA curves of the polyacrylate nanoparticles [P(BA–MMA)s] and PNLs containing 20, 30, and 40% lilial theoretically. The pure polyacrylate nanoparticles were decomposed completely between 320 and 400°C. All of the PNLs had two thermal decomposition periods, the first decomposition corresponded to lilial, and the second one corresponded to P(BA–MMA). Relative to the pure polyacrylate, the weight loss of the first decomposition of the PNLs increased with increasing lilial loading content. The first weight loss of the PNLs with 20% lilial in theory was 17.94%, that with 30% lilial was 23.39%, and that with 40% lilial was 36.83%. The efficiency of the fragrance encapsulation depended on the miniemulsion polymerization process with a homogeneous mixture of the dispersed phase consisting of the monomer, the fragrance, the surfactant, hexadecane as an osmotic pressure agent, and KPS as a hydrophilic initiator.[15]

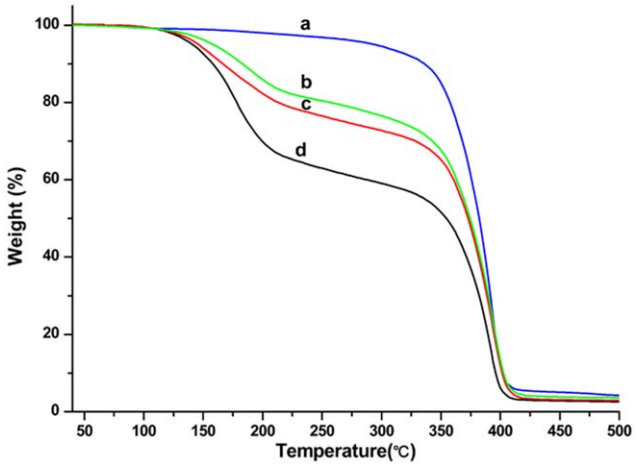

Figure 5. TGA results: (a) P(BA–MMA), (b) PNL with 20% lilial loading, (c) PNL with a 30% lilial loading, and (d) PNL with a 40% lilial loading. [Color figure can be viewed in the online issue, which is available at wileyonlinelibrary.com.]

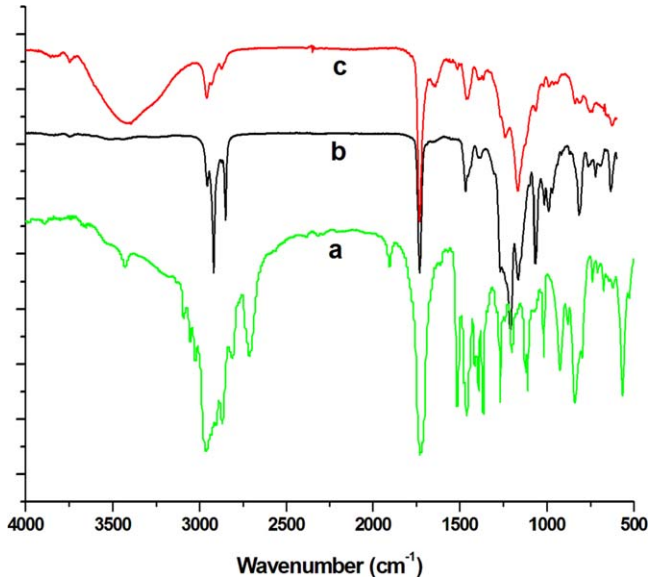

Figure 6. FTIR results: (a) lilial, (b) P(BA-MMA), and (c) PNL. [Color figure can be viewed in the online issue, which is available at wileyonlinelibrary.com.]

FTIR Spectroscopy Results

Figure 6 presents the FTIR spectra of P(BA–MMA), PNLs, and lilial. For the P(BA–MMA) nanoparticles, the characteristic absorption band ranging from 1150 to 1200 cm^{-1} was attributed to the stretching vibrations of the C—O groups of polyacrylate. Although the absorption band at 1731 cm^{-1} was assigned to the stretching vibrations of C═O groups, and the band ranging from 2800 to 2900 cm^{-1} was attributed to the alkyl vibration. In addition, the absence of the characteristic absorption band of —C═C— groups at 1600–1700 cm^{-1} showed that the monomers were polymerized completely. The lilial exhibited its characteristic absorption peaks at 1726 cm^{-1}, which were assigned to the —C═O group, and 3100–3000 cm^{-1}, which were attributed to the benzene ring. The obtained PNLs displayed not only these characteristic absorption bands of polyacrylate but also absorption peaks from 3100 to 3000 cm^{-1}, which were attributed to the benzene ring of lilial. However, the obvious absorption peak of the —OH group at 3397 cm^{-1} appeared in the PNL because of some water present in the samples.

TEM and DLS Results

Figure 7 shows the micromorphology and size distribution of the PNLs. DLS results based on statistics theory show that the mean size of the PNLs was 67.78 nm and the polydispersity index was 0.076. The TEM image shows that the spherical PNL dispersed unevenly; the minimum nanocapsule diameter was about 30 nm, and the maximum reached 80 nm. Because of the limits of the emulsifiers, some acrylate monomers could not diffuse into the micelles, so they were polymerized to form polyacrylate nanoparticles. So some small black round particles were P(BA–MMA).

Formation Mechanism of the Lilial Nanocapsules

According to the previous experimental phenomena and explanations, the formation mechanism of PNL was determined as follows. At first, lilial and hexadecane as water-insoluble materials

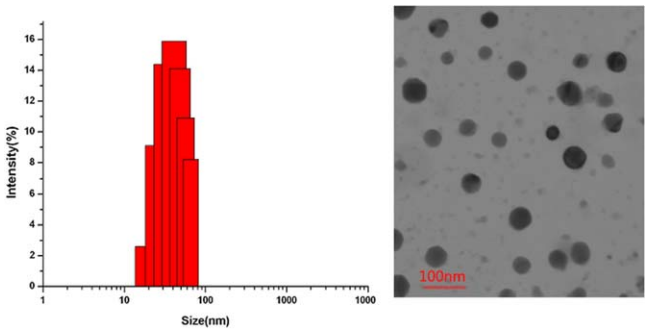

Figure 7. TEM and DLS results of the PNL. [Color figure can be viewed in the online issue, which is available at wileyonlinelibrary.com.]

were emulsified by the surfactants under strong mechanical action in the aqueous phase, so the O/W miniemulsion was obtained. When acrylate monomers were added to the system, they were diffused into the micelles through the aqueous phase. KPS as the water-soluble initiator produced the free-radical groups in the aqueous phase directly. So the acrylate monomers with double bonds existing the O/W interface were first polymerized to form the wall of the encapsulated lilial micelles initiated by KPS. When the acrylate monomers at the interface were consumed completely, those in the interior of the micelles migrated to be polymerized. Therefore, the polyacrylate nanocapsule encapsulated lilial was obtained. The formation mechanism of the nanocapsule is illustrated in Figure 8. On the other hand, some P(BA–MMA) particles, as shown in Figure 7, were also present in the whole system. In this experiment, it was difficult for too many acrylate monomers to be completely solubilized in the micelles formed by the surfactants. The solubility of MMA in water was 0.15 mol/L (45°C), and that of BA was 0.01 mol/L (45°C).[21] So the excess acrylate monomers partly dissolved or formed monomer droplets in the aqueous phase. With the initiation of KPS, MMA and BA dissolved in water were first copolymerized to form a P(BA–MMA) oligomeric radical. The acrylate monomers in the monomer droplets continued to react with the oligomeric radicals. At last, the P(BA–MMA) particles were prepared.

SEM Analysis

Figure 9(a,b) shows the surface appearances of the untreated leather fibers. The leather was a kind of three-dimensional

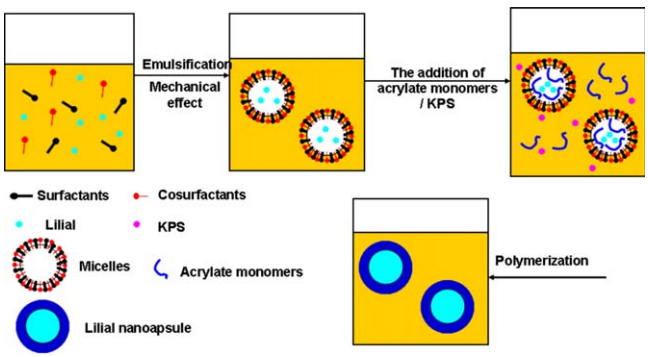

Figure 8. Formation mechanism of the PNL. [Color figure can be viewed in the online issue, which is available at wileyonlinelibrary.com.]

retiform structure, composed of collagen fiber bundles. The untreated leather collagen fibers exhibited a uniform neat gridding structure, and its surface was smooth. When the leather was treated with the lilial emulsion and PNLs, respectively, the surface of the leather became coarse, and some spherical particles adhered on the surface of the leather fibers, as shown in Figure 9(c,e). The lilial emulsion particles on the leather fibers were small, about 100–200 nm. Although the size of PNL aggregated on the surface of the leather fibers increased to 200–300 nm. This was attributed to the fact that the encapsulated shell P(BA–MMA) of the PNL retained a high elastic state. After they were flexed 5000 times, small or no residual lilial emulsion particles remained on the fiber surface; this showed the limited retention of a trace amount of lilial because of the weak physical function between the lilial emulsion particles and the fibers [Figure 9(d)]. However, there was a big aggregation of particles dispersed on the surface of the leather finished by the PNLs [Figure 9(f)]. Although the mechanical function decreased the amount of PNLs on the leather, there were a lot of PNLs on the surface of the leather fibers. For this reason, the P(BA–MMA) shell of the PNLs was a kind of sticky organic resin, and it interacted easily with the leather fibers. Meanwhile, the PNLs in the high elastic state collapsed to form a big aggregation under the strong mechanical reaction.

Release of the Lilial from the Finished Leather

The release of the lilial from the leather finished by lilial emulsion and the PNLs was determined, as shown in Figure 10. When the leathers finished by the lilial emulsion and the PNLs were flexed 5000 times, the aromatic strength of both finished leathers declined. When the nanocapsules were crushed and pressed, the elastic polyacrylate shell was squeezed, and the fragrance was released. The fragrance of the finished leather with lilial emulsion after it was flexed 5000 times decreased by 26.53%, whereas that with PNLs after it was flexed 5000 times declined by 7.24%. This illustrated that the polyacrylate nanocapsule encapsulated with lilial had excellent sustained release properties.

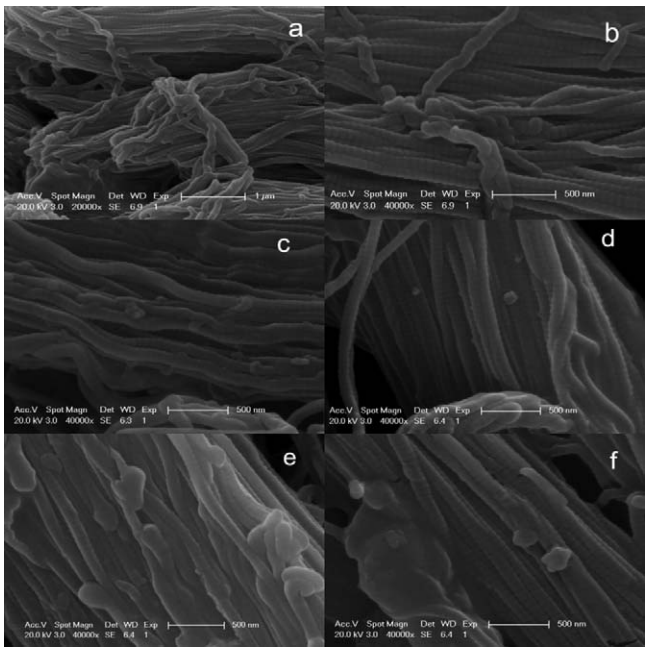

Figure 9. SEM results of the (a,b) untreated leather, (c,d) leather finished by lilial emulsion, and (e,f) PNL (c,e) without flexing and (d,f) after flexing 5000 times.

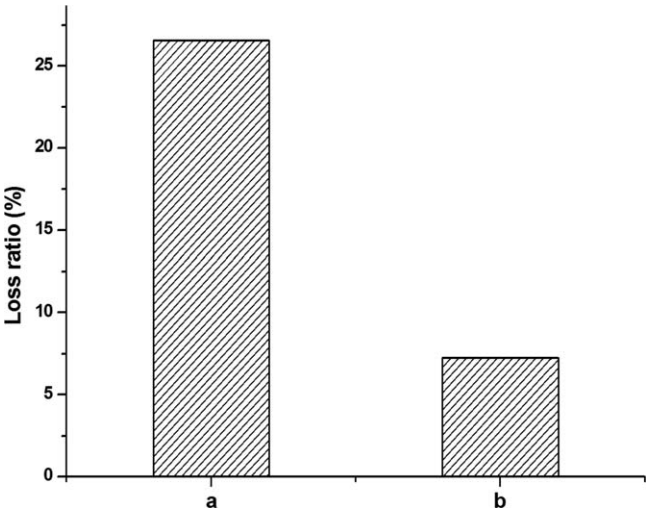

Figure 10. GC-FID result of the leather finished by (a) lilial emulsion and (b) PNL.

CONCLUSIONS

A higher loading ratio of the PNLs was prepared via miniemulsion polymerization with a shell of polyacrylate. The contents of the surfactants and lilial and the stirring speed obviously influenced the size and lilial loading capacity of the PNLs. DLS showed that the mean size of the PNLs was 67.78 and the polydispersity index was 0.076. TEM illustrated that the size of the spherical PNLs varied in the range 30–80 nm. TGA showed that the PNLs had two periods of thermal decomposition, which corresponded to the lilial and polyacrylate. With increasing lilial content, the first weight loss of the PNLs was improved. This showed that more lilial could be encapsulated into the nanocapsules. FTIR spectroscopy demonstrated that lilial was encapsulated into the polyacrylate nanocapsule successfully. SEM showed that there were some PNLs on the surface of the leather finished by the PNLs after it was flexed 5000 times. However, with the PNLs, it was easy to assemble the big particle after the strong mechanical actions belonging to the high elastic state of PNL. GC-FID indicated that the strength of the fragrance released from the leather finished by lilial emulsion after it was flexed 5000 times decreased by 26.53%, whereas that with only PNLs decreased by 7.24%. We verified that the PNLs had an excellent fragrance sustained release properties.

ACKNOWLEDGMENTS

Financial support from the National Natural Science Foundation of China (contract grant number 21106084), Innovation Program of Shanghai Municipal Education Commission (contract grant numbers 12YZ158 and 14zz164), and Shanghai Postdoctoral Science Foundation (contract grant number 13R21410500) is greatly appreciated.

REFERENCES

1. Herrmann, A. *Angew. Chem. Int. Ed.* **2007**, *46*, 5836.
2. Madene, A.; Jacquot, M.; Scher, J.; Desobry, S. *Int. J. Food Sci. Technol.* **2006**, *41*, 1.
3. Yang, J.; Xiao, J. X.; Ding, L. Z. *Eur. Food Res. Tech.* **2009**, *229*, 467.
4. Céline, T.; Georg, K.; Christopher, J. G. P.; Tuan, Q. N.; Andreas, H.; Lahoussine, O.; Horst, S.; Wolfgang, F.; Maria, I. V.; Harm-Anton, K.; Jan-Anders, E. M. *Macromol. Chem. Phys.* **2007**, *208*, 131.
5. Helena, M. C. M. *Flavour Fragr. J.* **2010**, *25*, 313.
6. Pranee, L.; Pornchai, R.; Ubonthip, N. *Mater. Sci. Eng. C* **2009**, *29*, 856.
7. Pranee, L.; Khanittha, N.; Nutthapon, J.; Pornchai, R.; Ubonthip, N. *Carbohydr. Polym.* **2008**, *74*, 209.
8. Brückner, M.; Bade, M.; Kunz, B. *Eur. Food Res. Technol.* **2007**, *226*, 137.
9. Hong, J.; Park, S. *Mater. Chem. Phys.* **1999**, *58*, 128.
10. Ouali, L.; Latreche, D. U.S. Pat US7279542 B2 (**2007**).
11. Feczkó, T.; Kokol, V.; Voncina, B. *Macromol. Res.* **2010**, *18*, 636.
12. Hwang, J. S.; Kim, J. N.; Wee, Y. J.; Yun, J. S.; Jiang, H. J.; Kim, S. H.; Ryu, H. W. *Biotech. Bioprocess. Eng.* **2006**, *11*, 4.
13. Wang, P.; Zhu, Y. H.; Yang, X. L.; Chen, A. P. *Flavour Fragr. J.* **2008**, *23*, 29.
14. Seemork, J.; Tree-Udom, T.; Wanichwecharungruang, S. *Flavour Fragr. J.* **2012**, *27*, 386.
15. Landfester, K.; Musyanovych, A.; Volker, M. V. *J. Polym. Sci. Part A: Polym. Chem.* **2010**, *48*, 493.
16. Landfester, K. *Angew. Chem. Int. Ed.* **2009**, *48*, 4488.
17. Theisinger, S.; Schoeller, K.; Osborn, B.; Sarkar, M.; Landfester, K. *Macromol. Chem. Phys.* **2009**, *210*, 411.
18. Hu, J.; Xiao, Z. B.; Zhou, R. J.; Li, Z.; Wang, M. X.; Ma, S. S. *Flavour Fragr. J.* **2011**, *26*, 162.
19. Hu, J.; Xiao, Z. B.; Ma, S. S.; Zhou, R. J.; Wang, M. X.; Li, Z. *J. Appl. Polym. Sci.* **2012**, *123*, 3748.
20. Park, Y. H.; Baek, N. J.; Kim, Y. J. *J. Kor. Fiber Soc.* **2001**, *38*, 589.
21. Aslamazova, T. R. *Prog. Org. Coatings* **1995**, *25*, 109.